

Supporting Information

Prolonged near-infrared fluorescence imaging of microRNAs and proteases in vivo by aggregation-enhanced emission from DNA-AuNCs nanomachines

Ting Wang,^a Kai Jiang,^a Yifan Wang,^a Limei Xu,^a Yingqi Liu,^a Shiling Zhang,^a Weiwei Xiong,^a Yemei Wang,^a Fenfen Zheng,^{*,a} Jun-Jie Zhu^{*,b}

Author affiliation

^aSchool of Environmental & Chemical Engineering, Jiangsu University of Science and Technology, Changhui Rd. 666, Zhenjiang, Jiangsu 212003, China.

^bState Key Laboratory of Analytical for Life Science, School of Chemistry and Chemical Engineering, Nanjing University, Xianlin Ave 163, Nanjing, Jiangsu 210023, China

Email: zhengfenfen@just.edu.cn; jjzhu@nju.edu.cn

Table of Contents

1. Experimental procedures	
Chemicals	S4
Table S1	S4
Instrumentation	S4
Synthesis of AuNCs	S5
Synthesis of DNA-AuNCs Nanomachine	S5
Synthesis of Cat B responsive DpAuNC8 or DpAuNC6 nanomediators	S6
TK1 mRNA detection by mDNA-AuNCs nanomachines	S6
The responsiveness of DpAuNC8 to Cat B	S6
Cat B detection by DpAuNC8 and pDNA-AuNC8 cascade nanomachines	S6
Polyacrylamide gel electrophoresis	S6
Cell Culture	S7
Cell uptake of the nanomachines	S7
In Vitro Cytotoxicity of the Nanomachines	S7
Intracellular Imaging of TK1 mRNA	S8
Intracellular fluorescence imaging of Cat B activity	S8
In vivo imaging	S9
Biodistribution of the nanomachines in mice	S9
Renal clearance of the nanomachines in mice	S9
Statistical Analysis	S9
2. Supplementary Figure S1-S23	
Figure S1. UV-vis absorption spectra of AuNC6, mDNA-AuNC6 and TK1 mRNA+mDNA-AuNC6 solution	S10
Figure S2. Zeta potential monitoring of the assembly processes of mDNA-AuNC6	S10
Figure S3. Fluorescent spectra of mDNA-AuNC6 with different mTD concentrations in the presence of TK1 mRNA	S11
Figure S4. Emission spectra of mDNA-AuNC6 in the presence of TK1 mRNA for different incubation time	S11
Figure S5. UV-vis absorption spectra of AuNC8, pAuNC8 and DpAuNC8 solution	S12
Figure S6. Polyacrylamide gel electrophoresis (PAGE) analysis of Cat B-initiated TMSD	S12
Figure S7. Hydrodynamic diameter of pDNA-AuNC8+DpAuNC8, pDNA-AuNC8+DpAuNC8+Cat B	S13
Figure S8. Fluorescence emission spectra of pDNA-AuNC8 in the presence of different concentrations of initiator DNA	S13
Figure S9. Fluorescence emission spectra of pDNA-AuNC6+DpAuNC6 with increasing concentrations of Cat B	S14
Figure S10. The relationship between the fluorescent intensity at 605 nm and different concentrations of Cat B. Error bars show the standard deviations of three experiments	S14
Figure S11. Fluorescence emission spectra of mDNA-AuNC8 with different TK1	

mRNA concentrations.....	S15
Figure S12. The relationship between the fluorescent intensity at 826 nm and different concentrations of TK1 mRNA. Error bars show the standard deviations of three experiments	S15
Figure S13. Relative viabilities of 4T1 cells after incubation with different nanosystems	S16
Figure S14. Fluorescence images of 4T1 cells co-stained with calcein AM/PI after being treated with different formulations. The Scale bar represents 100 μm	S16
Figure S15. Internalization study of the nanomachines by quantifying intracellular Au amount	S17
Figure S16. In vivo fluorescence images of 4T1 tumor-bearing mice without probe injection	S17
Figure S17. In vivo fluorescence images of 4T1 tumor-bearing mice obtained at different time after injection of AuNC6	S18
Figure S18. (a,b,c) Fluorescence intensities of the tumor sites treated with mDNA-AuNC6 (a), mDNA-AuNC6-R (b) and AuNC6 (c). (d,e,f) Contrast between tumor and skin of mDNA-AuNC6 (d), mDNA-AuNC6-R (e) and AuNC6 (f)	S19
Figure S19. (a) Ex vivo fluorescence images of 4T1 tumor-bearing mice at 24 h intravenous post-injection of mDNA-AuNC6 or mDNA-AuNC6-R. (b) The fluorescence intensities of tumor and main organs in (a)	S19
Figure S20. Au content in urine sample collected after administration of the nanomachines for different time	S20
Figure S21. Contrast between tumor and skin of mDNA-AuNC8-R or mDNA-AuNC8	S20
Figure S22. (a) In vivo fluorescence images of 4T1 tumor-bearing mice obtained at different time after injection of cascade probe, cascade probe+inhibitor or cascade probe+stimulator. (b) Fluorescence intensities of the tumor sites in (a)	S21
Figure S23. Histological analysis of the normal tissues after treatment with the nanomachines	S21
3. References	S21

1. Experimental procedures

Chemicals

GSH, $\text{HAuCl}_4 \cdot 3\text{H}_2\text{O}$ and anhydrous ethanol were purchased from Sinopharm Chemical Reagent Co., Ltd. (Shanghai, China). Cathepsin B and its inhibitor, antipain hydrochloride, were purchased from Sigma-Aldrich (Shanghai, China). 3-(4,5-Dimethylthiazol-2-yl)-2,5-diphenyltetrazolium bromide (MTT), doxorubicin (Dox), 4',6-diamidino-2-phenylindole (DAPI), Lyso-Tracker Green and the annexin V-FITC apoptosis detection kit were obtained from KeyGen Biotech. Co. Ltd. (Nanjing, China). Gel electrophoresis loading buffer and ladder DNA were purchased from ThermoFisher Scientific Co. Ltd. (USA). Phosphate buffer saline (PBS, 10 mM, pH 7.4) contained 136.7 mM NaCl, 2.7 mM KCl, 8.7 mM Na_2HPO_4 and 1.4 mM KH_2PO_4 . All other reagents were of analytical grade and used without purification. The used peptides were purchased from GL Biochem Ltd. (Shanghai, China). The sequences are as follows: CRRGGKKGKRRK.

All the oligonucleotides used here were synthesized and purified by Sangon Biotechnology Co. Ltd. (Shanghai, China), and all the oligonucleotide sequences are listed in Table S1.

Table S1. Sequences of synthesized oligonucleotides.

Name	DNA sequence (5'-3')
The sequence of TK1 mRNA	5'-CAA GUA UGC CAA AGA CAC UCG C-3'
the responsive substrate of TK1 mRNA	mA: 5'- GCG AGT GTC TTT GGC ATA CTT GTC AAG GCC GTA AGT TGT GTT T-SH-3' C:5'- ACA CAC AAC TTA CGG-3' mD: 5'-CCC AGC CTT CCA GCT CCT TGA CAA GTA TGC CAA AGA C-3' mFD: 5'-ACT AAC TTA CGG CCT TGA CAA GTA TGC CAA ATT T-SH-3'
the responsive substrate of Cat B	Mediator DNA: 5'-CCGAGTGTCTTTGGCATACTTG-3' pA : 5'-CAA GTA TGC CAA AGA CAC TCG GTC AAG GCC GTA AGT TGT GTT T-SH-3' pD:5'-CCC AGC CTT CCA GCT CCT TGA CCG AGT GTC TTT GGC A -3' pFD:5'-CTC AAC TTA CGG CCT TGA CCG AGT GTC TTT GTT T-SH-3'

Instrumentation

The UV-Vis absorption spectra were recorded on a UV-Vis spectrometer UV-3600 (Shimadzu, Japan). Fluorescence spectra were conducted on a F-7000 spectrofluorophotometer (Shimadzu Co. Japan). Transmission

electron microscopy (TEM) images were recorded by a JEOL-2010 transmission electron microscope (JEOL, Japan). The concentration of nanomachine (Au) was measured by an inductively coupled plasma optical emission spectrometer (ICP-OES, Agilent Technologies). A BIO-RAD ChemiDoc XRs was used for polyacrylamide gel electrophoresis (PAGE) imaging. The Dynamic light scattering (DLS) experiments and zeta potential was obtained on a 90 plus (Brookhaven Instruments, USA). Fluorescent microscopy studies were acquired using an Olympus IX73 inverted fluorescent microscope (Germany). MTT assay was recorded at 490 nm using a microplate reader (SpectraMax i3, Molecular Devices). The fluorescence images of the mice were performed using a FOBI in vivo imaging system.

Synthesis of AuNCs

The AuNCs with emission at 605 nm (AuNC6) were synthesized based on previous methods.¹ Typically, 20 μ L of 1 M $\text{HAuCl}_4 \cdot 3\text{H}_2\text{O}$ and 300 μ L of 100 mM GSH were added into 9.7 mL of deionized water and homogenized well. The mixture was then heated to 70 °C and reacted for 24 hours under slow stirring. The resulting solution emitted orange fluorescence and the solution was re-dissolved in deionized water followed by dialysis using a dialysis bag (retained molecular weight: 1000 Da). The obtained AuNC6 solution could be stored at 4 °C for 2 months with negligible change in their optical properties. Similarly, the preparation method of AuNCs with emission at 826 nm (AuNC8) is as follows,² 17 mL of 2.4 mM GSH is heated to 95 °C in an oil bath and stabilized for 30 min, and then reacted with 50 μ L of 1 M $\text{HAuCl}_4 \cdot 3\text{H}_2\text{O}$ for 35 min. The resulting solution was mixed with twice the volume of acidic ethanol and centrifuged, washed with deionized water for three times, and finally re-suspended in PBS (PH=7) and stored at 4 °C.

Synthesis of DNA-AuNC Nanomachines

To construct mDNA-AuNCs that responds to TK1 mRNA, mTD and mFD were conjugated to the AuNC6 (mDNA-AuNC6) or AuNC8 (mDNA-AuNC8) through Au-S bonds, where mTD chain was hybridized with mA, C, and mD chains. Before use, DNA modified with thiol groups was activated for 40 min with TCEP (50 mM). Then, 10 μ L of SH-mA (100 μ M), 10 μ L of C (100 μ M), and 10 μ L of mD (100 μ M) were heated to denaturation to obtain SH-mTD. Finally, 100 μ M SH-mTD and 100 μ M SH-mFD were mixed with 500 μ L of AuNC6 or AuNC8 and homogenized by vortexing. The mixture was then stored in a refrigerator at -20°C for 2 hours before being centrifuged to remove free DNA. To remove the unreacted DNA the obtained mDNA-AuNC nanomachines were purified by dialysis in nanopure water. The resulting DNA-AuNCs were stored at 4°C for further use. Similarly, pDNA-AuNC (including

pDNA-AuNC8 and pDNA-AuNC6) nanomachines for Cat B detection are prepared using the above method, but pA, pD, pFD and were used instead of mA, mD, mFD, respectively.

Synthesis of Cat B responsive DpAuNC8 or DpAuNC6 nanomediators

The peptides were conjugated on the surface of AuNCs by Au-S bond. 500 μL of AuNC8 or AuNC6 (2 mg mL^{-1}) was mixed with 100 μL of SH-functionalized peptide (5 mg mL^{-1}). The mixture was stirred at 4°C for 48 h to form the peptide-functionalized AuNC8 or AuNC6 (pAuNC8 or pAuNC6). The resulting nano particles were centrifuged and thoroughly washed with PBS (10 mM, pH 7.4) to remove the unreacted peptide. Next, the mediator DNAs were assembled on the surface of the pAuNC8 or pAuNC6 through electrostatic interaction. Specifically, 50 μL of 100 μM mediator DNA solution was added to 1 mL of 0.5 mg pAuNC8 or pAuNC6, and the mixture was shaken at room temperature for 30 minutes. The mixture was then centrifuged at 9500 rpm for two times to obtain the Cat B responsive nanomediators (DpAuNC8 or DpAuNC6).

TK1 mRNA detection by mDNA-AuNC nanomachines

Different concentrations of TK1 mRNA were added into 500 μL of aqueous solution containing mDNA-AuNCs (DpAuNC8 or DpAuNC6). After stirring for 4 h at 37°C , the desired aggregation of mDNA-AuNCs was observed. The fluorescence spectra of the samples were measured and recorded.

The responsiveness of DpAuNC8 to Cat B

To demonstrate the release of FAM-labeled mediator DNAs from the DpAuNC8 nanomediators in response to Cat B, the fluorescence recovery of the nanomediators in the presence of commercial Cat B standard with different concentrations was measured after incubation at 37°C for 30 min.

Cat B detection by DpAuNC8 and pDNA-AuNC8 cascade nanomachines

Similar to the aggregation response to TK1 mRNA, 30 μL of Cat B at different concentrations were added into 100 μL of the mixture of DpAuNC8 nanomediators (0.1 mg mL^{-1}) and pDNA-AuNC8 nanomachines (0.1 mg mL^{-1}) at 37°C for 4 hours. The resulting mixture was immediately measured for fluorescence. Fluorescence spectroscopy was performed using a F-7000 fluorescence spectrophotometer (Hitachi, Japan) under excitation at 600 nm. The slit width was set to 10 nm for both excitation and emission.

Polyacrylamide gel electrophoresis

The 10% native polyacrylamide gel electrophoresis (PAGE) was used to verify the reaction feasibility of the mDNA-AuNC nanomachines at room temperature for 1 hour at a constant voltage of 100 V, 50 mA. The 1~5 lanes correspond to C, mA, mFD, TK1 mRNA, and mD respectively. The 7 lane is the mTD hybrid band formed after incubating mA, mC, and mD at 37°C for 1 hour in PBS. lane 8 is the band formed after incubating mTD, mFD, and target TK1 mRNA at 37°C for 1 hour in the mixture. Lane 10 is the band formed after incubating mTD and mFD in the mixture for 1 hour. Lane 9 is the band formed after incubating mA and mFD for 1 hour. Lane 7 can be clearly observed the mTD hybrid band, while lane 9 show clear mA/mFD band. After incubation with the target, lane 8 also shows obvious mA/mFD band, proving the released mD band through the TMSD reaction. The feasibility of pDNA-AuNC nanomachines for Cat B detection was also validated by PAGE, just using pA, pD and pFD to instead mA, mD and mFD, respectively.

Cell Culture

Mice breast cancer cell line 4T1, human cervical cancer cell line HeLa, and mouse fibroblast cell line NIH-3T3 were all purchased from KeyGen Biotech. Co. Ltd. (Nanjing, China). NIH-3T3 or HeLa cell were cultured in DMEM culture medium supplemented with 10% fetal bovine serum at 37 °C in a humidified 5% CO₂ incubator. 4T1 cells were cultured in RPMI-1640 medium supplemented with 10% FBS and Penicillin-Streptomycin solution (100 U/mL and 100 µg/mL, respectively).

Cell uptake of the nanomachines

The 4T1 cells were cultured in four-well glass bottom plates at a density of 10000 cells/well in each well overnight. Then the cells were incubated with fresh culture media containing mDNA-AuNC6 at 37°C for different time. Next, the cells were washed with PBS, and digested with EDTA-trypsin. After that, the cells were rinsed with PBS and boiled in chloro-nitric acid for 24 hours, and then the solution was evaporated completely. Finally, 4 mL 2% nitric acid was added to the cells. The resulted solution was passed through a 0.22 µm filter membrane for processing. The content of Au in the solution was measured by ICP-OES and the amount of Au in cells was calculated.

In Vitro Cytotoxicity of the Nanomachines

MTT assay was used to study the cytotoxicity of different concentrations of mDNA-AuNC6 or DpAuNC8 plus pDNA-AuNC8 on cancer cells. In brief, the 4T1 cells were cultured in a 96-well plate with a density of 10000 cells/well for overnight. Cultured medium containing different concentrations of samples was added to each

well. After incubation for 24 h, removed the medium of each well, and fresh medium (100 μL) containing MTT (10 μL , 5 mg mL^{-1}) was added into each well to form formazan. After 4 h of incubation, 100 μL of DMSO was added to each well. Finally, the OD value was measured at 490 nm. The results were expressed as the mean values of three measurements.

The cell death was also assessed via Calcein AM/propidium iodide (PI) co-staining methods. Typically, the 4T1 cells were cultured in four-well glass bottom plates at a density of 10000 cells/well in each well overnight. The medium was replaced with fresh complete medium containing samples with different formulations. After incubation for 24 h, the medium was removed, and the cells were washed three times with PBS, then resuspended in 200 μL of medium containing Calcein-AM and PI and incubated at 37 $^{\circ}\text{C}$ in the dark for 30 minutes. After that, the cells were washed with PBS and supplemented with fresh culture medium for further imaging.

Intracellular Imaging of TK1 mRNA

4T1 cells, HeLa cells and 3T3 cells (1×10^5 cells) were respectively incubated with mDNA-AuNC6 nanomachines for different time at 37 $^{\circ}\text{C}$, followed by washing three times with 1 mL of PBS (10 mM, pH 7.4) and adding fresh medium. Then, the cells were observed using fluorescent microscopy. To study the distribution of DNA-AuNCs in 4T1 cells, HeLa cells, and 3T3 cells, cells were stained with Hoechst 33342 and LysoTracker green. Briefly, 150 μL of Hoechst and Lyso Tracker solution was mixed with 4T1 cells, HeLa cells, and 3T3 cells which were treated with mDNA-AuNC6 nanomachine and incubated at 37 $^{\circ}\text{C}$ for 30 min. Then, the cells were washed with PBS buffer and added in fresh medium for microscopic observation. All cellular fluorescent images were collected on an Olympus IX73 inverted fluorescence microscope.

Intracellular fluorescence imaging of Cat B activity

Fluorescence imaging of intracellular Cat B activity was performed as follows. The 4T1 cells were inoculated onto a four-well glass bottom plate at a density of 10,000 cells/well and were allowed to attach for overnight. Prior to incubation with the Cat B responsive DpAuNC8 nanomediators and pDNA-AuNC8 nanomachines, the cells were pretreated with Cat B inhibitor or Cat B stimulator for 2 hours. Then the cells were washed twice with PBS (pH=7.4, 10 mM) and cultured with fresh culture medium containing both DpAuNC8 nanomediators and DNA-AuNC8 nanomachines at 37 $^{\circ}\text{C}$ for 8 hours. Finally, the cells were washed three times with PBS and supplemented with fresh culture medium before imaging.

In vivo imaging

All animal studies were performed in accordance with the Jiangsu Animal Care and Use Committee (SYXK(Su)2023). To establish the tumor xenograft model, the female nude mice (4~6weeks) were inoculated with 4T1 cells (8×10^4 cells in 20 μ L of PBS) in their right thighs. For real-time monitoring of TK1 mRNA, the mice were intratumorally injected with mDNA-AuNC6, mDNA-AuNC6-R or mAuNC6 (50 μ L of 0.9 mg/mL (based on the mass of the AuNC6)), or intravenously injected with mDNA-AuNC8, mDNA-AuNC8-R (125 μ L of 0.9 mg/mL (based on the mass of the AuNC8)). For Cat B imaging, the mice were intratumorally injected with pDNA-AuNC8 and DpAuNC8 (50 μ L of 0.9 mg/mL (based on the mass of the AuNC8)) or intravenously injected with pDNA-AuNC8 and DpAuNC8 (125 μ L of 0.9 mg/mL (based on the mass of the AuNC8)) after pretreatment with Cat B inhibitor and stimulator. The real-time fluorescence imaging was carried out on a FOBI in vivo imaging system at different time points, respectively. Then the mice were euthanized, and the organs ((heart, liver, spleen, kidneys and lung) and tumors were collected for ex-vivo imaging using the same system.

Biodistribution of the nanomachines in mice

The tumor-bearing mice were injected with DNA-AuNCs by tail vein injected and then euthanized at specific time. The major organs (heart, liver, spleen, lung, and kidney) and tumors were collected and weighed. All tissues were digested in chloro-nitric acid for 24 h, then evaporated and mixed with 6 mL of 2% HNO₃ and centrifuged. The solution was passed through a 0.22- μ m filter membrane for processing. The concentration of Au in the solution was measured by inductively coupled plasma (ICP-OES) and the amount of Au in each tissue was calculated as a percentage of the injection dose per gram (%ID/g) for tumors and major organs.

Renal clearance of the nanomachines in mice

In order to further prove that mDNA-AuNC6 could accumulate and stay at the tumor site for a longer time after aggregation, mDNA-AuNC6, mDNA-AuNC6-R, AuNC6 were injected into mice by tail vein injection, and urine was collected for 4, 8, 12, and 24 h. Urine at different time points were digested in chloro-nitric acid for 24 h, then evaporated and mixed with 6 mL of 2% HNO₃ and centrifuged. The solution was passed through a 0.22- μ m filter membrane for processing. The concentration of Au in the solution was measured by inductively coupled plasma (ICP-OES).

Statistical Analysis

Data were expressed as mean \pm standard deviation (SD) and student's t-test was used to evaluate the significance of the difference. The difference was identified as significant when $P < 0.05$ (*) and very significant when $P < 0.01$ (**) or $P < 0.001$ (***).

2. Supplementary Figure S1-S23

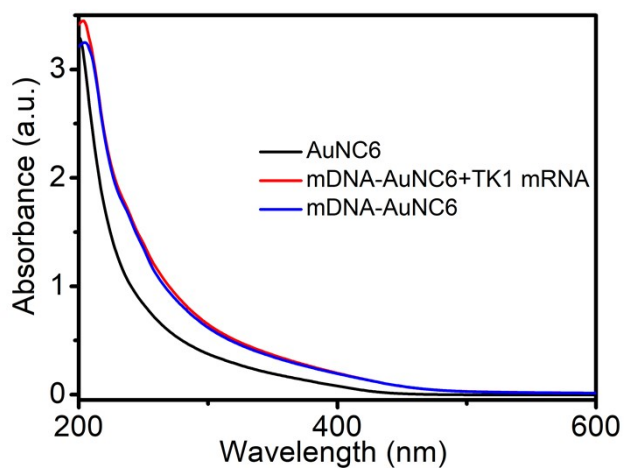


Figure S1. UV-vis absorption spectra of AuNC6, mDNA-AuNC6 and TK1 mRNA+mDNA-AuNC6 solution.

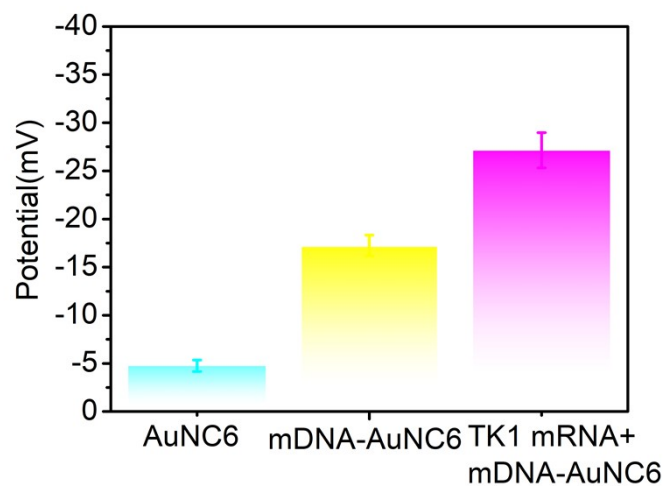


Figure S2. Zeta potential monitoring of the assembly processes of mDNA-AuNC6.

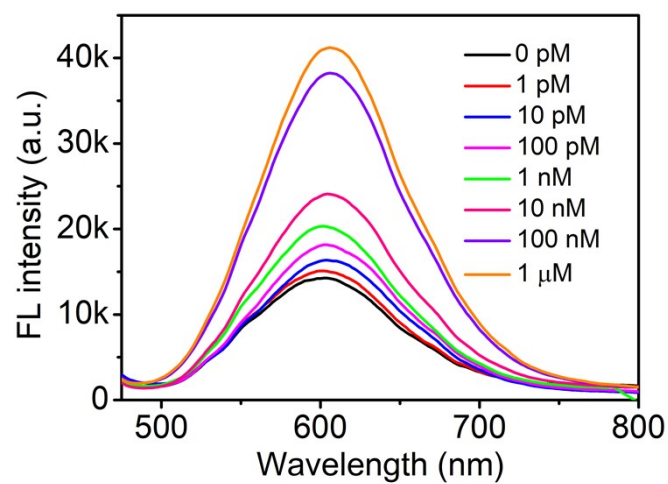


Figure S3. Fluorescent spectra of mDNA-AuNC6 with different mTD concentrations in the presence of TK1 mRNA.

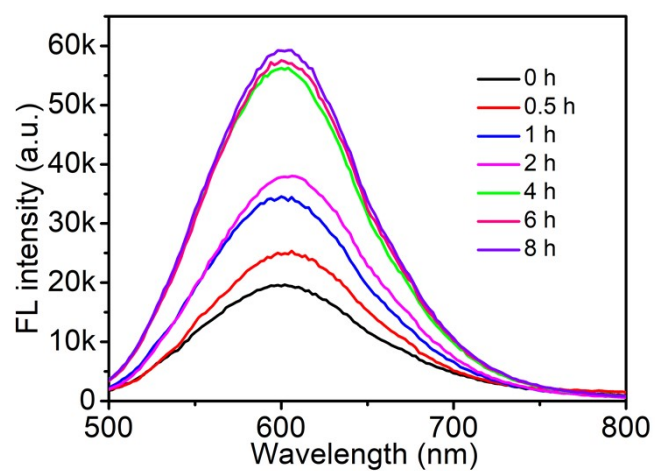


Figure S4. Emission spectra of mDNA-AuNC6 in the presence of TK1 mRNA for different incubation time.

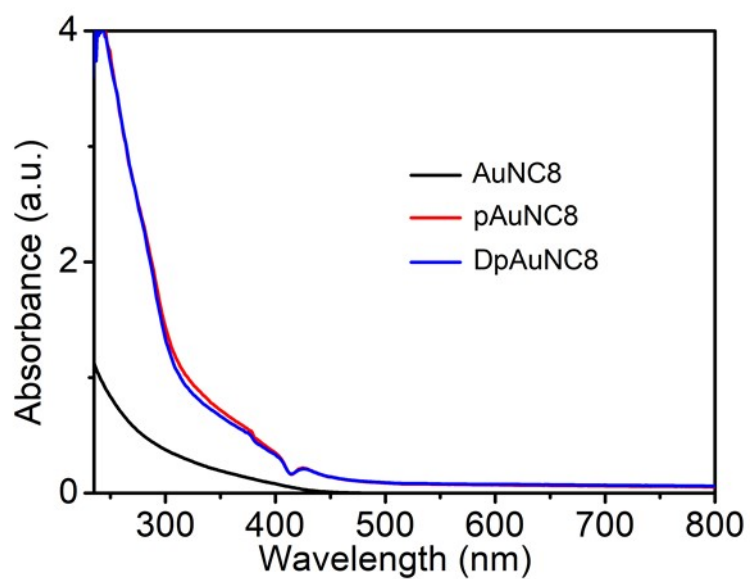


Figure S5. UV-vis absorption spectra of AuNC8, pAuNC8 and DpAuNC8 solution.

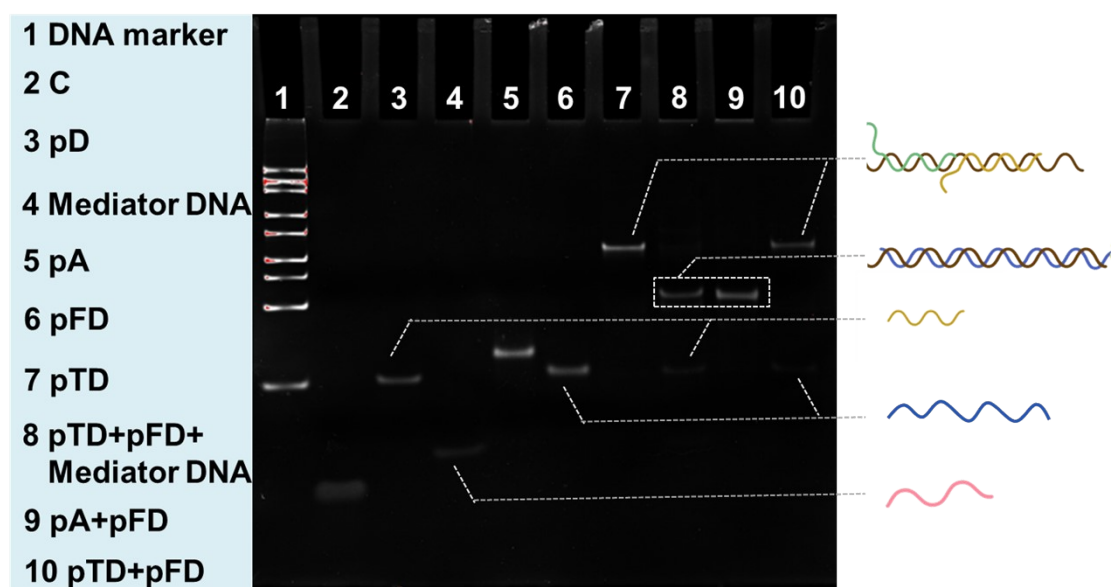


Figure S6. Polyacrylamide gel electrophoresis (PAGE) analysis of Cat B-initiated TMSD.

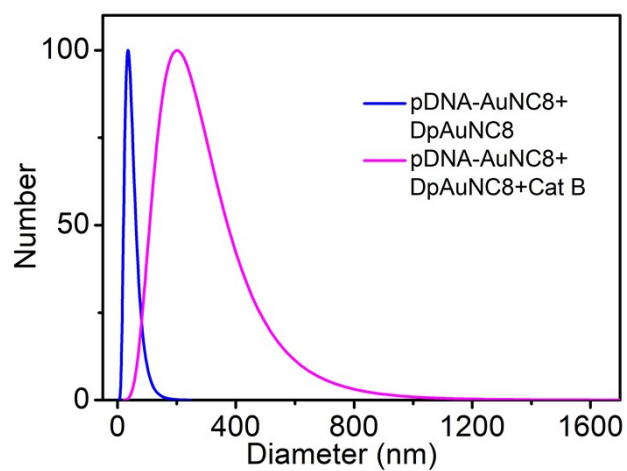


Figure S7. Hydrodynamic diameter of pDNA-AuNC8+DpAuNC8, pDNA-AuNC8+DpAuNC8+Cat B.

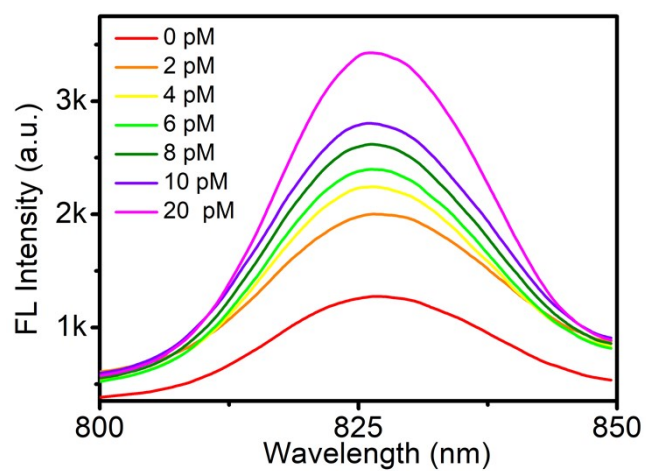


Figure S8. Fluorescence emission spectra of pDNA-AuNC8 in the presence of different concentrations of initiator DNA.

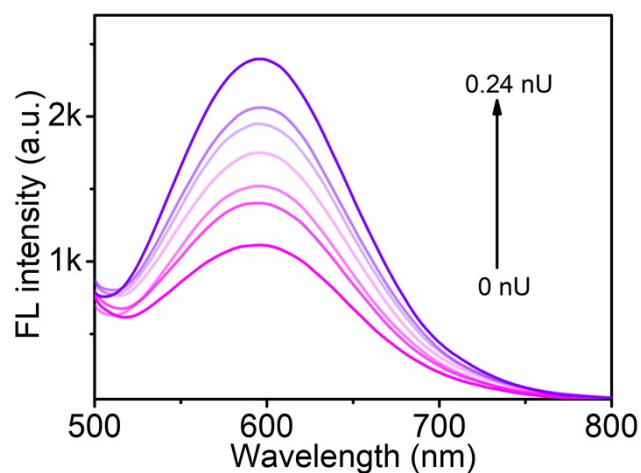


Figure S9. Fluorescence emission spectra of pDNA-AuNC6+DpAuNC6 with increasing concentrations of Cat B.

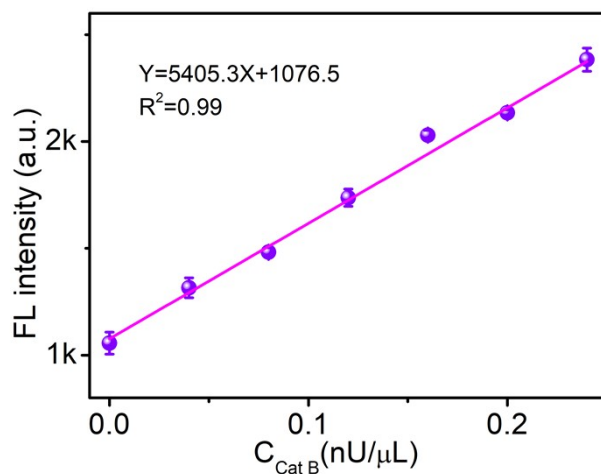


Figure S10. The relationship between the fluorescent intensity at 605 nm and different concentrations of Cat B. Error bars show the standard deviations of three experiments.

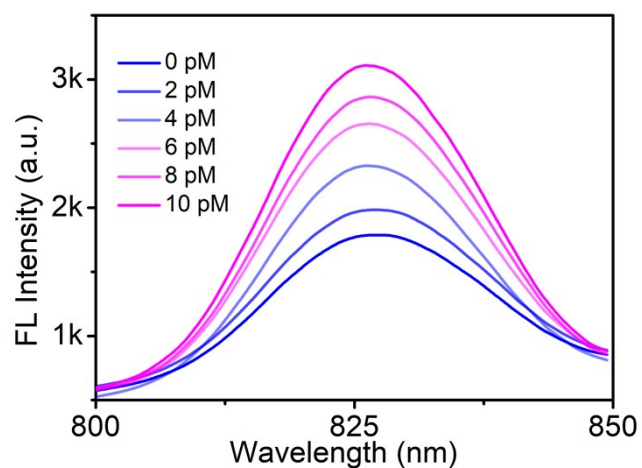


Figure S11. Fluorescence emission spectra of mDNA-AuNC8 with different TK1 mRNA concentrations.

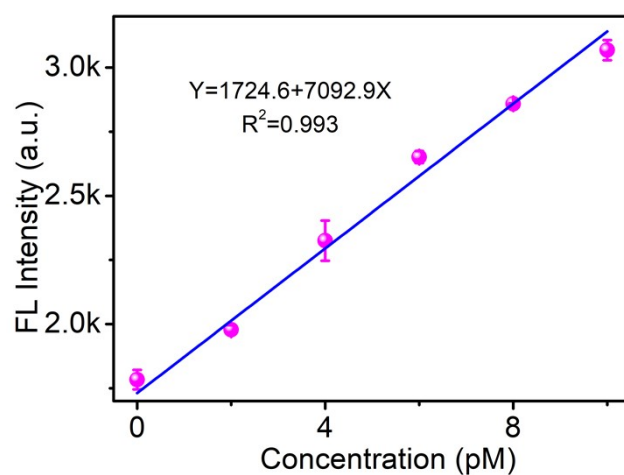


Figure S12. The relationship between the fluorescent intensity at 826 nm and different concentrations of TK1 mRNA. Error bars show the standard deviations of three experiments.

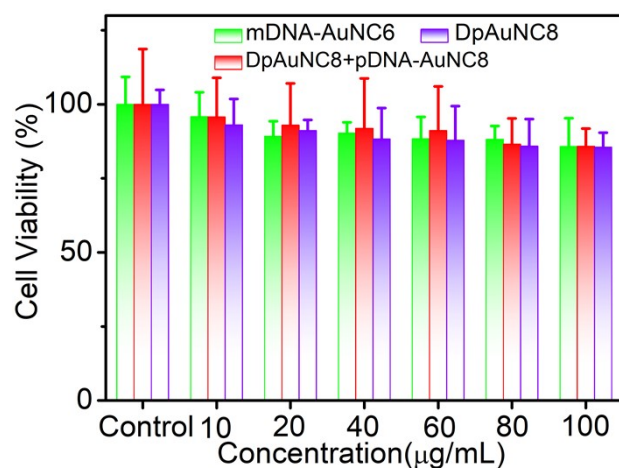


Figure S13. Relative viabilities of 4T1 cells after incubation with different nanosystems.

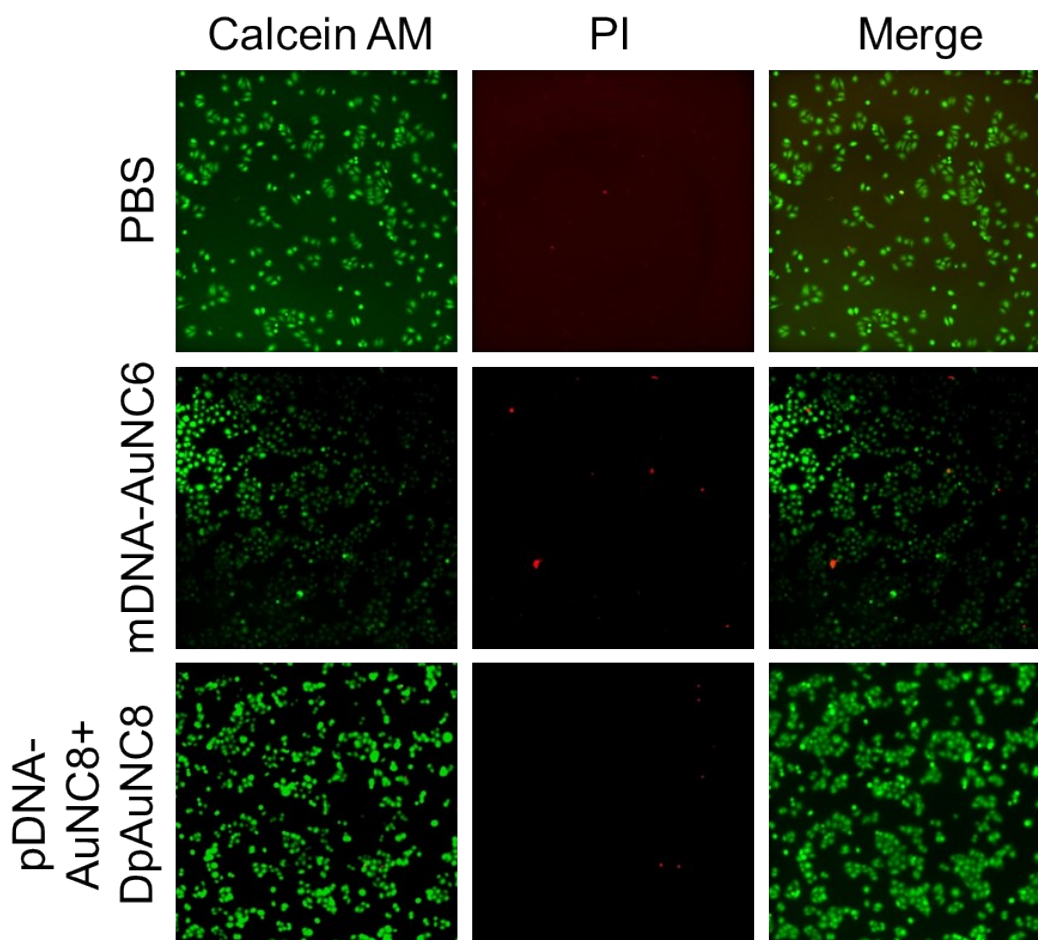


Figure S14. Fluorescence images of 4T1 cells co-stained with calcein AM/PI after being treated with different formulations. The Scale bar represents 100 µm.

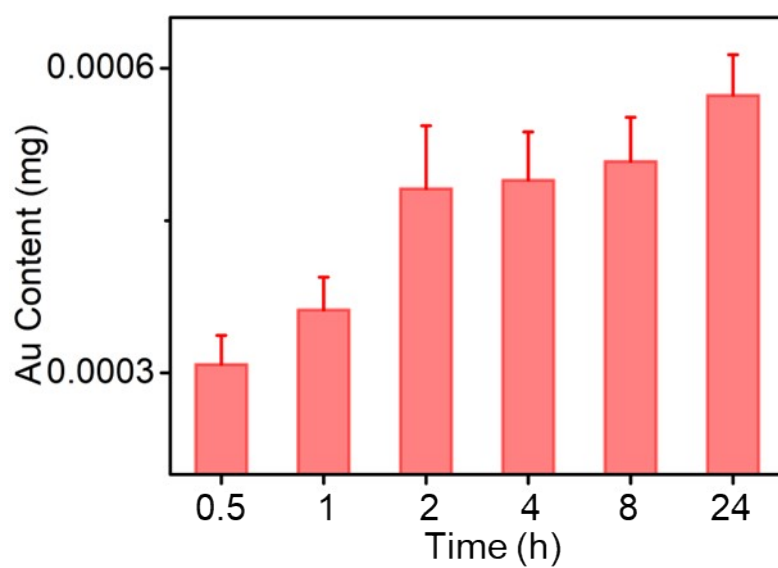


Figure S15. Internalization study of the nanomachines by quantifying intracellular Au amount.

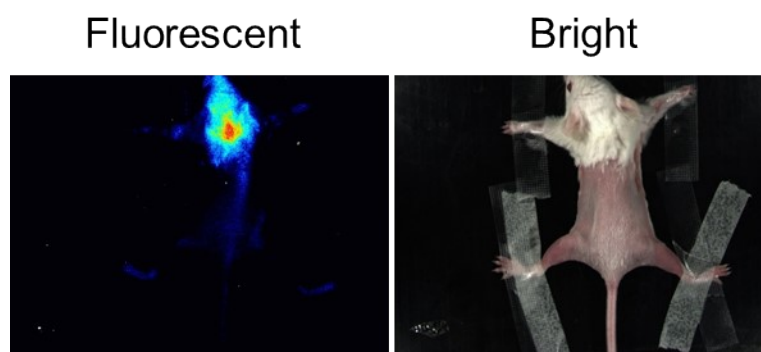


Figure S16. In vivo fluorescence images of 4T1 tumor-bearing mice without probe injection.

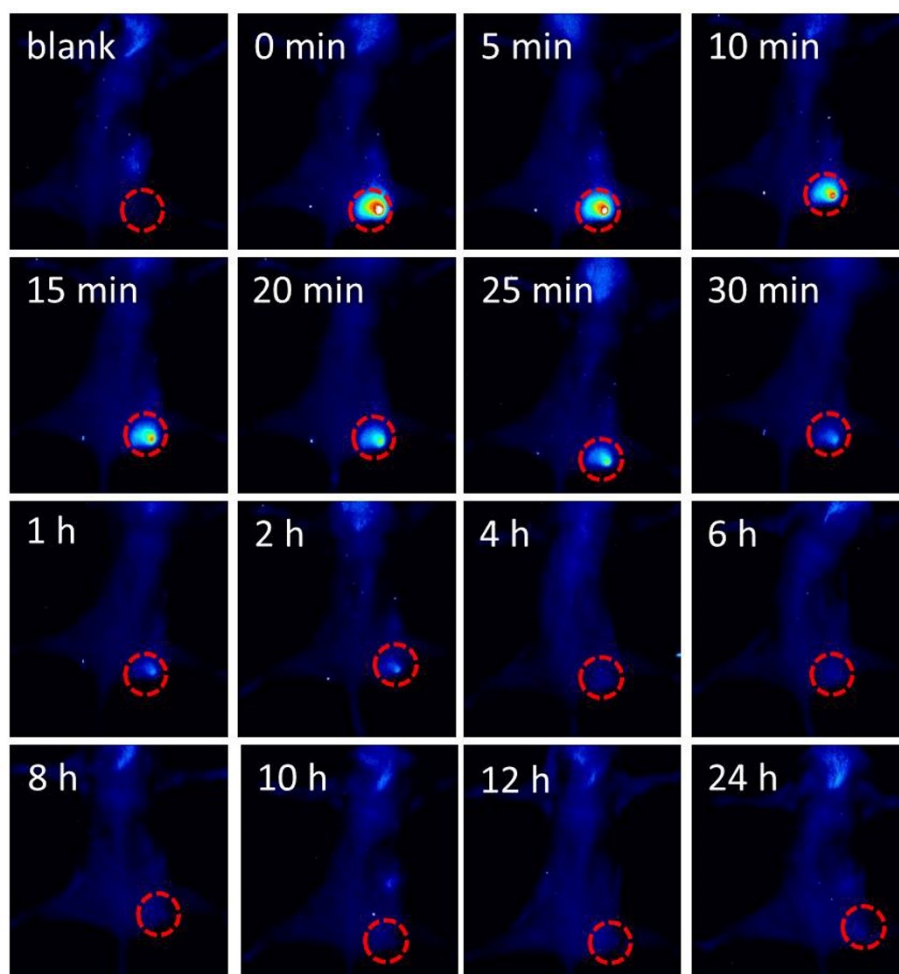


Figure S17. In vivo fluorescence images of 4T1 tumor-bearing mice obtained at different time after injection of AuNC6.

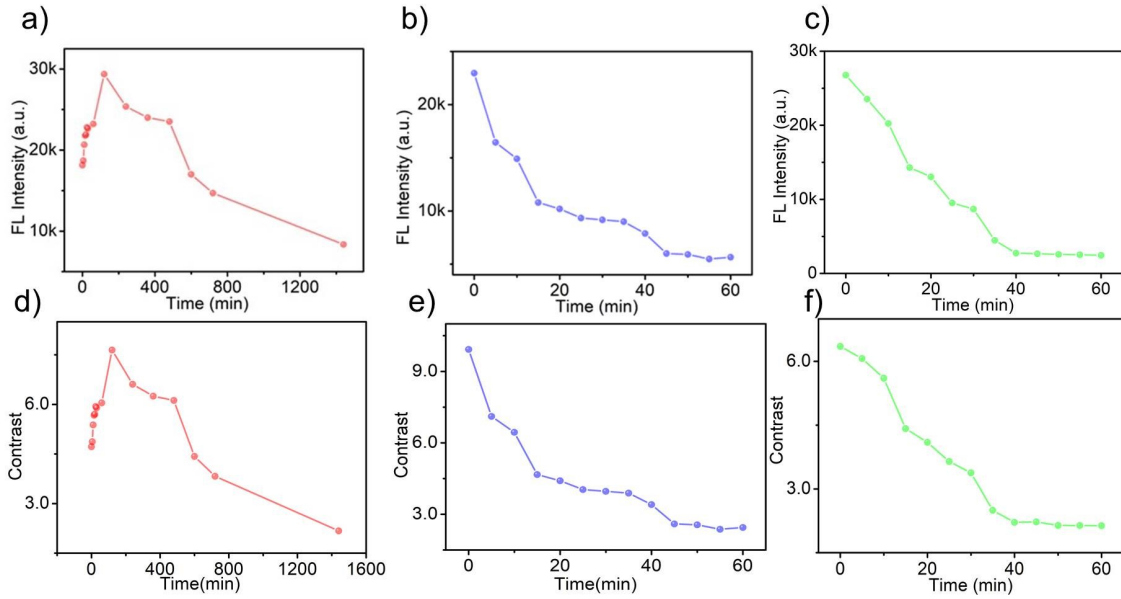


Figure S18. (a,b,c) Fluorescence intensities of the tumor sites treated with mDNA-AuNC6 (a), mDNA-AuNC6-R (b) and AuNC6 (c). (d,e,f) Contrast between tumor and skin of mDNA-AuNC6 (d), mDNA-AuNC6-R (e) and AuNC6 (f).

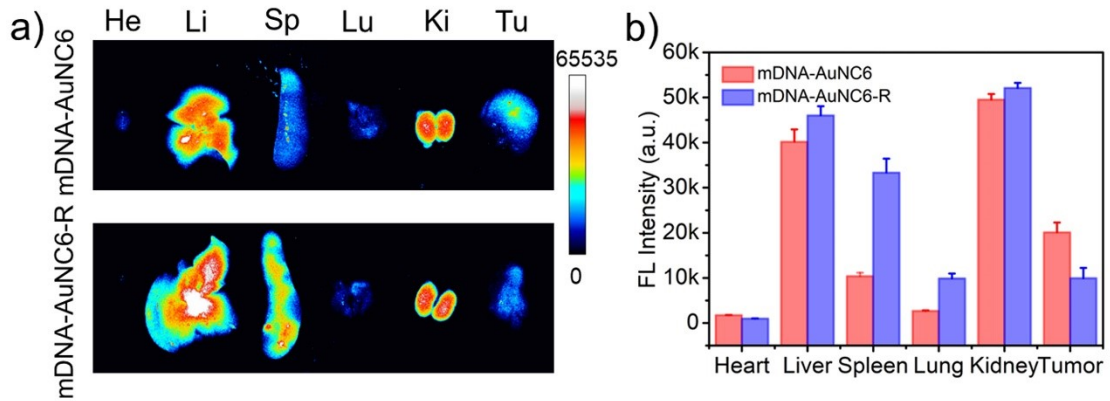


Figure S19. (a) Ex vivo fluorescence images of 4T1 tumor-bearing mice at 24 h intravenous post-injection of mDNA-AuNC6 or mDNA-AuNC6-R. (b) The fluorescence intensities of tumor and main organs in (a).

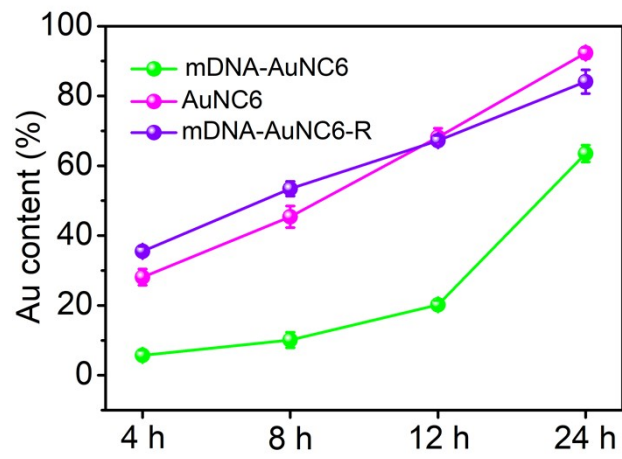


Figure S20. Au content in urine sample collected after administration of the nanomachines for different time.

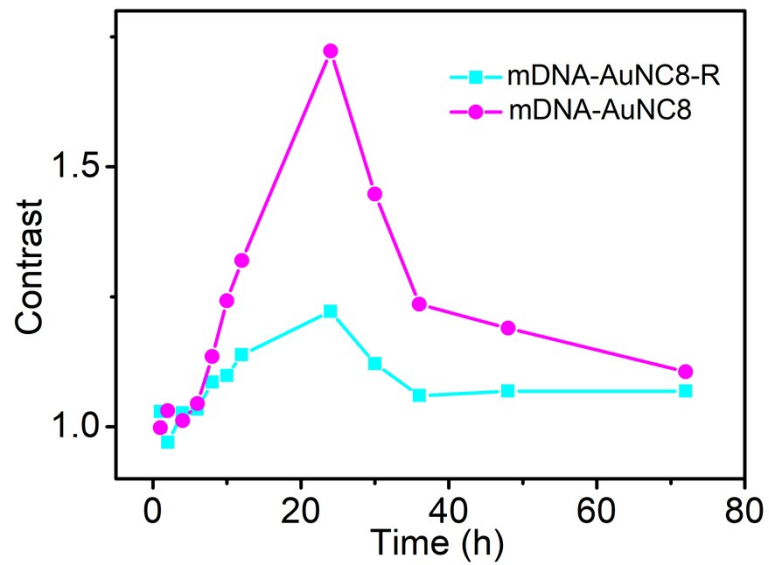


Figure S21. Contrast between tumor and skin of mDNA-AuNC8-R or mDNA-AuNC8.

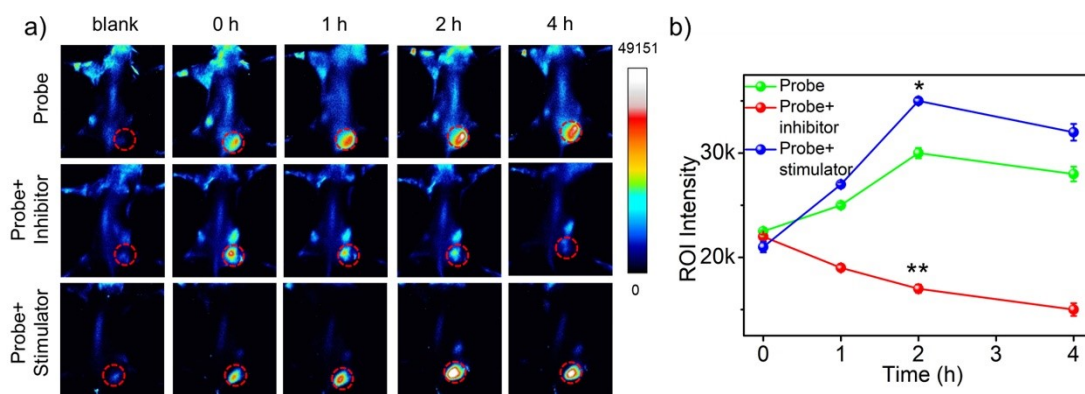


Figure S22. (a) In vivo fluorescence images of 4T1 tumor-bearing mice obtained at different time after injection of cascade probe, cascade probe+inhibitor or cascade probe+stimulator. (b) Fluorescence intensities of the tumor sites in (a).

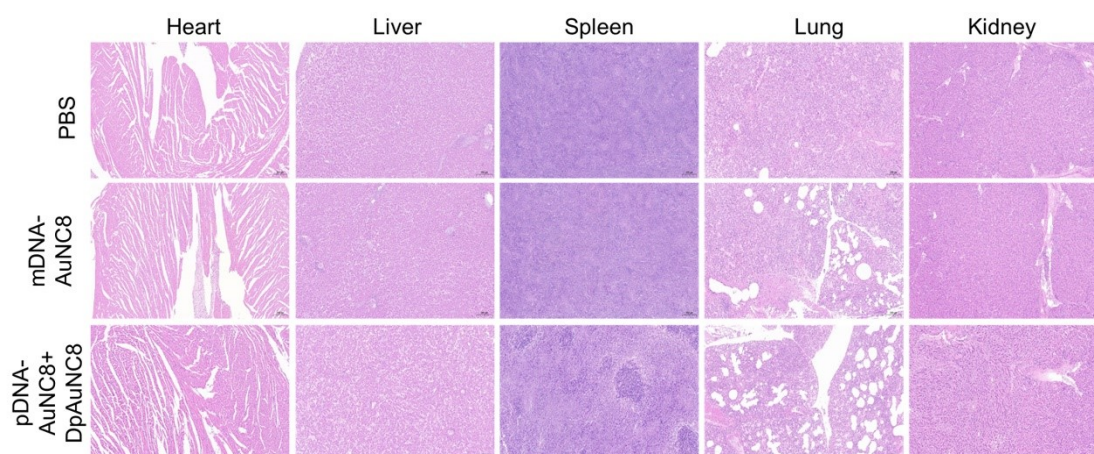


Figure S23. Histological analysis of the normal tissues after treatment with the nanomachines.

3. References

- 1 Zhang. H, Han. W, Cao. X, et al, *Microchim Acta*, 2019, **353**, 186.
- 2 Hada. AM, Craciun. AM, Focsan. M, et al, *Microchim Acta*, 2022, **337**, 189.